CFD simulations of a wind turbine for analysis of tip vortex breakdown

K Kimura[1], Y Tanabe[2], T Aoyama[2], Y Matsuo[2], C Arakawa[1] and M Iida[1]

[1] The University of Tokyo, 7-3-1 Hongo, Bunkyo-ku, Tokyo, 113-8656, Japan
[2] Japan Aerospace Exploration Agency, 7-44-1 Jindaijihigashimachi, Chofu-shi, Tokyo, 182-8522, Japan

E-mail: k.kimura@gg.cfdl.t.u-tokyo.ac.jp

Abstract. This paper discusses about the wake structure of wind turbine via the use of URANS and Quasi-DNS, focussing on the tip vortex breakdown. The moving overlapped structured grids CFD Solver based on a fourth-order reconstruction and an all-speed scheme, rFlow3D is used for capturing the characteristics of tip vortices. The results from the Model Experiments in Controlled Conditions project (MEXICO) was accordingly selected for executing wake simulations through the variation of tip speed ratio (TSR); in an operational wind turbine, TSR often changes in value. Therefore, it is important to assess the potential effects of TSR on wake characteristics. The results obtained by changing TSR show the variations of the position of wake breakdown and wake expansion. The correspondence between vortices and radial/rotational flow is also confirmed.

1. Introduction

For economical use of wind turbine, it is important to install the wind turbines collectively at one site (wind farm). The collective layout leads to good effects such as the reductions of the total length of power transmission lines, the load for maintenance etc... However, the wake behind the wind turbines is known to cause major problems when the turbines are in a collective layout. A wind turbine converts the kinetic energy of wind into mechanical energy; consequently, the speed of the wind in the wake region is greatly reduced. Moreover, the existence of tip vortices impedes momentum exchange between the wake and the main stream [1]. Therefore, it needs a long distance to recover the wake velocity. In addition, when these vortices directly flow in a subsequent wind turbine, its fatigue damage gets accumulated faster. For the above reasons, each wind turbine in a wind farm is placed away from the others. From past researches and some experiences, distance of 10D (D is the diameter of the wind turbines) between two rotors is recommended [2]. However, this criterion is determined empirically, and the optimum distance is supposed to vary depending on the operational conditions. Therefore, the wake structure must be investigated by using scientific approaches for the optimum layout of the wind farms.

Experimental or/and numerical approaches have been considered to study the wake structure. The experimental approaches' results typically tend to be reliable because it can deal with the actual phenomena. However, future commercial wind turbine becomes increasingly large, and experimentally performing the grasping of the flow will become difficult in view of the scaling law in the flow dynamics such as the Reynolds number problems. At present, the rotor diameters of the commercial wind turbines are approximately 100 m and will increase to approximately 200 m in the future, making it very

expensive to perform experiments. Alternatively, numerical studies do not require such construction costs. In addition, the entire field data can be obtained via computational fluid dynamics (CFD). At present, CFD can predict the average flow fields around the wind turbines and become a tool for understanding the wake structure. Vermeer *et al.* [3] summarized several methods of CFD for the wake simulation. They reported that Reynolds-averaged Navier-Stokes (RANS) simulation was able to give fair results in attached aerofoil flow conditions. On the other hand, Large Eddy Simulation (LES) or Detached Eddy Simulation (DES) were better to simulate separated aerofoil flow condition. Up to the present time, many researchers have developed the CFD methods for wake simulation and studied about various conditions to reproduce the detailed structure of wake. Troldborg *et al.* [4] investigated the effect of CFD models for wind turbine on the wake such as actuator disc (AD) and actuator line (AL) models. The distribution of vortices is greatly influenced by the type of rotor modelling and it is significant to resolve the rotor geometry for capturing the wake vortices. AbdelSalam *et al.* [5] also reported the advantages of fully resolving the rotor geometry in terms of prediction of the wake velocity. Modelling of the natural wind is also important to simulate actual operations. Li *et al.* [6] have implemented the velocity fluctuations into the inflow condition to model the natural wind. Considering the disturbance of the natural wind, it is understood that wake recovery gets faster than uniform flow.Nilay *et al.* [7] have studied the effect of wind shear on wake flow structure. The existence of a wind sheer causes vortices become close each other, which increases the mutual interaction between vortices. These CFD results can be used to develop wake models oriented to predict velocity deficits. Göçmen *et al.* [8] reviewed the wake models developed at DTU. Compared with the field test and CFD results, they show the availability of the wake models for considering the wind farm layout in terms of velocity deficits. Although wake models are getting reliable to use in industry, it has a difficulty for reproducing the values of velocity deficit when inflows fluctuate and the turbulence intensity get increased. To be more precise, understanding and modelling of vortex breakdown is important because it generates a large velocity gradient. Discussion on the behaviour of the tip vortices is ongoing and it needs to be solved by using CFD.

In this study, the CFD simulations of the wind turbine were conducted to study the vortex structure and the breakdown process by using a higher order scheme and dynamic calculations. To consider various operational conditions, the tip speed ratio λ (TSR) is changed and the simulations are executed. It is carried out to investigate the relation between TSR and the tip vortex structures.

2. Approach

2.1. Case study

The model wind turbine that was previously used in the Model Experiments in Controlled Conditions (MEXICO) project, was selected as case study [9-12]. One of the special features of this test is that it includes particle image velocimetry (PIV) measurements of near-wake regions. Therefore, such data can be used to validate CFD results of velocity distributions and/or vorticity distributions. The specifications for the MEXICO experiment are shown in table 1. The Reynolds number is based on the characteristic chord length (at 82% spanwise position) and the rotational speed of blade tip. Several researchers have previously endeavoured to simulate the MEXICO rotor by CFD. For example, Micallef *et al.* [13] studied the effects of yawed conditions on wake characteristics and Carrion *et al.* [14] executed TSR cases of MEXICO using a compressible multi block solver and an all-Mach scheme; both of their calculations ultimately reproduced the flow around the MEXICO rotor with precision. Moreover, Réthoré *et al.* [15] investigated wind tunnel effects on wake characteristics in MEXICO experiments, concluding that the impact of wind tunnels on wakes is not significant in PIV measurement region.

Table 1. Specifications of MEXICO experiments [9].

Rotor diameter (D) [m]	4.5
Number of blades [-]	3
Speed of main flow[m/s]	10, 15, 24
Tip speed ratio [-]	10, 6.67, 4.17
Rated rotational speed [rpm]	424.5
chord length [m]	0.113 (at 82% span-wise position)
Reynolds number	8×10^5

2.2. Analysis code

The Moving Overlapped Structured Grids CFD Solver rFlow3D [16] is used for wake analysis. rFlow3D was developed by the Japanese Aerospace eXploration Agency (JAXA) for analysing rotorcrafts such as helicopters. The governing equations are the compressible Navier–Stokes equations, which are discretised using a finite volume method (FVM). rFlow3D can address moving overlapped grids; thus, it can simulate the blade rotations and deformations. By using an all-speed numerical scheme SLAU [17], dissipations in low-speed area such as root of blades can be kept small. Furthermore, rFlow3D is good at capturing the blade tip vortices by adapting a fourth order reconstruction method FCMT [16]

2.3. Computational grid

The Computational grid is composed of two background Cartesian grids and three rotating blade grids for analysis. Furthermore, an inner background grid, which has high grid resolution was established to capture the small structure of the tip vortices. The grid covers from 0.5 rotor diameters upwind of the rotor plane to 10 rotor diameters downwind. Details of the computational grids are presented in table 2 and figure 1. x, y and z denote the axial, horizontal and vertical direction each other. The origin of the coordinate is the rotational canter of the wind turbine.

Table 2. Computational grid information.

	Blade Grid	Inner Background Grid	Outer Background Grid
Number of partition (x×y×z)	$121 \times 121 \times 61$	$1307 \times 187 \times 187$	$151 \times 101 \times 101$
Computational domain[a]	-	$10.5D \times 1.3D \times 1.3D$	$14.5D \times 5D \times 5D$
Minimum space[b]	$y^+ \approx 1$	0.32 c	0.32 c
Total number of cells	900 thousands	46 millions	1.5 millions

[a] diameter of the rotor D = 4.5 [m].
[b] chord length c = 0.113 [m] (at 82% span-wise position).

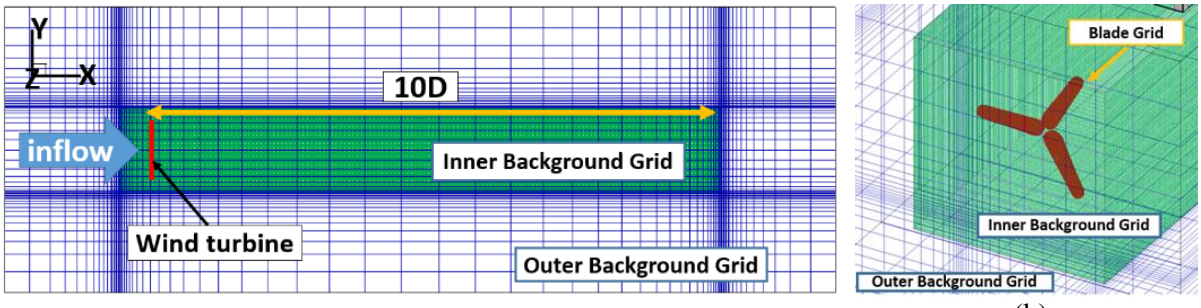

(a) (b)

Figure 1. Computational grid (a) wake region and (b) around Blade region.

2.4. Numerical analysis condition

In MEXICO experiments, tripping tape is used to transient from laminar to turbulent on blades [9]. Therefore, attached flows are expected in high TSR conditions and uses of turbulence model is considerable. However, such RANS simulations have difficulty for prediction of separated aerofoil flows. When TSR decreases, attached flow on the blades becomes separated flow because of increase the angle of attack. According to Tanabe *et al*. [18], some turbulence models of RANS tend to predict attached flows till a higher angle of attack. Therefore, In high TSR condition, RANS simulation should fail to reproduce the actual phenomena. To simulate separated flows, Quasi Direct Numerical Simulation (QDNS) is effective [18]. The QDNS does not use any turbulence model and it is utilized for capturing vortices of wake region [19]. In this study, Unsteady RANS (URANS) simulation with the Spalart-Allmaras (SA) turbulence model [20] and QDNS of the wind turbines were executed. The numerical analysis conditions are shown in table 3. A fourth-order compact MUSCL TVD [16] interpolation scheme was adopted as the reconstruction method. Thus, the resolution in space is fourth-order, enabling us to precisely capture even small vortices. The operational conditions are summarized in table 4. Please note that the inflow is uniform and steady.

Table 3. Numerical analysis condition.

Governing equations	Unsteady Reynolds-averaged Navier-Stokes equation / Navier-Stokes equation
Space discretization	Cell-vertex FVM (Background)/Cell-centered FVM (Blade Grid)
Inviscid flux	SLAU [17]
Reconstruction	4th order Compact MUSCL TVD interpolation [16]
Turbulence model	Spalart-Allmaras [18] / without turbulence model (Quasi-DNS)
Rotation of wind turbine	Moving Overlapped Structured Grids
Time integration	4th order Runge-Kutta (Background) LU-SGS/LU-DUR implicit method (Blade Grid)

Table 4. summary of computation in this study

case	Inflow speed [m/s]	Tip speed ratio [-]	Simulation model
1	10	10	URANS (SA)
2	15	6.67	URANS (SA)
3	24	4.17	URANS (SA)
4	24	4.17	QDNS

3. Comparison of macro characteristics

First, results must be validated by comparing them with results of the first MEXICO project experiments. Hence, three cases were simulated with $\lambda = 4.17, 6.67$ and 10, which are the conditions of MEXICO. The axial velocity along the span wise position (r = 1.8) at an azimuth angle of 270° is shown in figure 2. The results of New MEXICO [12], which was carried out to validate the previous MEXICO measurement, are plotted together with the MEXICO findings. Therefore, the specifications such as blade length are same as MEXICO experiment. As for $\lambda = 6.67$, which is the design point of the MEXICO rotor, although the URANS result slightly over predicts the velocity deficit around the rotor position (x/D = 0), it shows good agreement with both MEXICO and New MEXICO in the wake region. The simulation for the case of $\lambda = 10$ also predicted the velocity deficit well even around the rotor position (x/D = 0). However, the URANS simulation of the case of $\lambda = 4.17$ tends to over predict the velocity deficit. As mentioned in subsection 2.4, this tendency can be caused by the attached flow

predicted by SA model. As a result of attached flow, velocity deficit and force acting on the blade are overestimated. On the other hand, the results of QDNS shows good agreement with MEXICO results.

Next, the axial force distributions along the blade are shown in figure 3. Axial force is directly related to velocity deficit. Spanwise positions and axial force distributions are normalised by the rotor radius and dynamic pressure of inflows respectively. The magnitude of axial force is proportional to rotational speed; thus, axial force is found to increase as the radial position moves towards the tip. In contrast, axial force is found to sharply decrease around the blade tip because of tip loss. Focusing on each TSRs, the URANS simulations of $\lambda = 6.67$ and $\lambda = 10$ show good agreement with the MEXICO results qualitatively. However, these simulations slightly overestimate MEXICO results. This tendency could be caused by fully turbulent assumption of URANS, while tripping tape was used for laminar-turbulent transition in MEXICO rotor [21]. Same as the axial velocity, the URANS simulations of $\lambda = 4.17$ is found to over predict the axial force and QDNS shows consistency between MEXICO results.

From these two points of view (velocity deficit, axial force), it was determined that, in this study, the URANS and QDNS simulations successfully captured the basic characteristics of wind turbine wake. However, it should be necessary for the low-TSR case to adjust the numerical conditions.

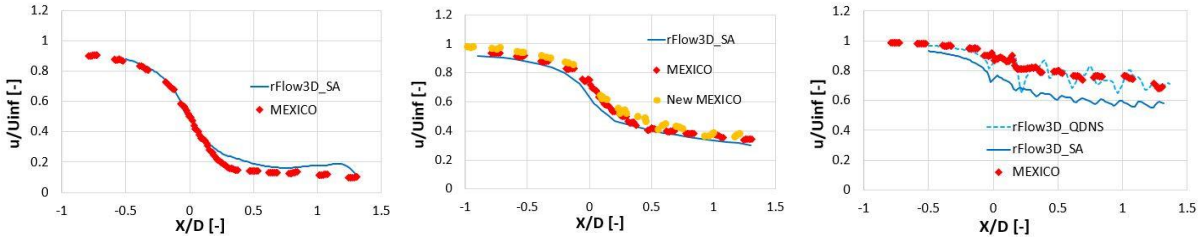

$u = 10$ m/s, $\lambda = 10$ $u = 15$ m/s, $\lambda = 6.67$ $u = 24$ m/s, $\lambda = 4.17$

Figure 2. Axial traverse of axial velocity[9,12]

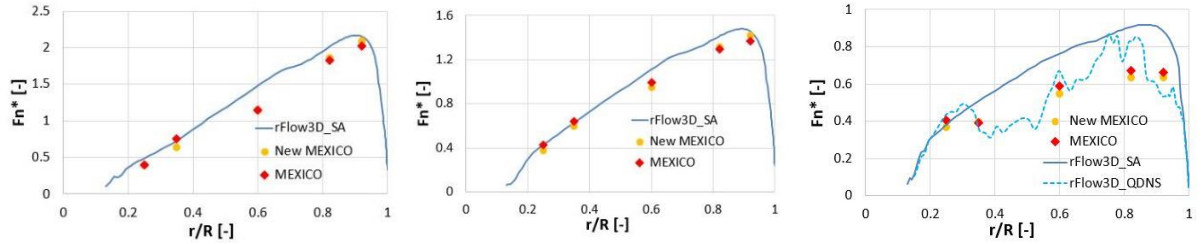

$u = 10$ m/s, $\lambda = 10$ $u = 15$ m/s, $\lambda = 6.67$ $u = 24$ m/s, $\lambda = 4.17$

Figure 3. Radial distribution of axial force along with blade [9,12]

4. Analysis of wake structure

4.1. Wake expansion and vortex breakdown

Further, analysis of vortex was executed to focus on the relationship between the vortices dynamics and TSR. As for $\lambda = 4.17$, please note that the result of QDNS simulation is used for analysis from this section because QDNS shows better agreement with MEXICO. The positions of the vortex core are shown in figure 4. The results of rFlow3D found to reproduce the MEXICO experiments with precision. When TSR increases, the radial expansion of tip vortices becomes greater. This behaviour is supposedly caused by changing the ratio of centrifugal force to wake velocity. Moreover, the radial expansion of wake should involve the vortex instability. The iso-surface of vorticity and the vorticity contour are shown in figures 6 and 7, respectively. Vorticity is normalised by the chord length in table 1 and the axial velocity of the main stream in each case. In general, the tip vortices are stable and minute structures do not exist at the initial stage of the wake. Subsequently, the vortices begin to interact with one another

and short wavelength instabilities appear. Finally, the helical structures completely break down. Similarly, root vortices are combined with each other and resultantly diffuse into the entire wake region. Following this phenomenon, tip and root vortices merge and ultimately shape the complex structure. Such actions correspond to mixing behaviours with the main stream.

The space between each vortex decreases as TSR increases. Consequently, the interaction of the vortices as a whole ultimately increases. For the case of $\lambda = 4.17$, the wake disturbance begins at the rotor position (x = 0) and the vortex core is maintained at x ≅ 2D. In this case, mid-span vortex is found as well as tip and root vortices. Mid-span vortex should be caused by separation flow. For $\lambda = 6.67$, however, the disturbance begins at x ≅ 1D and the vortices start to combine with each other. Around x ≅ 3D, the vortices become minute structure and vorticities become weak. and for $\lambda = 10$, the vortex combination begins at about x ≅ 0.25D, with the helical structure ultimately broken at x ≅ 1D. Subsequently, wake diffusion occurs and is greatly diffused prior to x = 2D. Each of these cases depicts a 'similar' process with regard to the vortex breakdown phenomena. In terms of attached flow conditions, However, the vortex breakdown is accelerated by an increasing TSR.

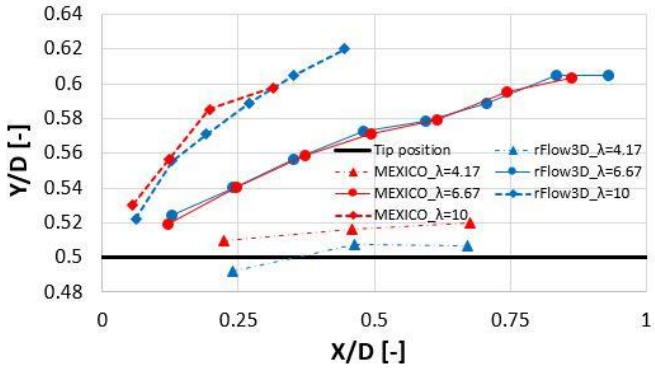

Figure 4. Positions of tip vortex core.[9]

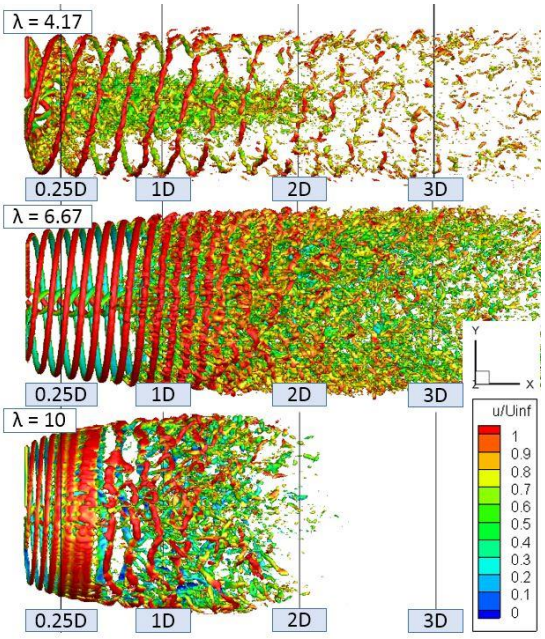

Figure 5. Iso-surface of normalized vorticity = 0.5 (top: $\lambda = 4.17$, middle: $\lambda = 6.67$, bottom: $\lambda = 10$).

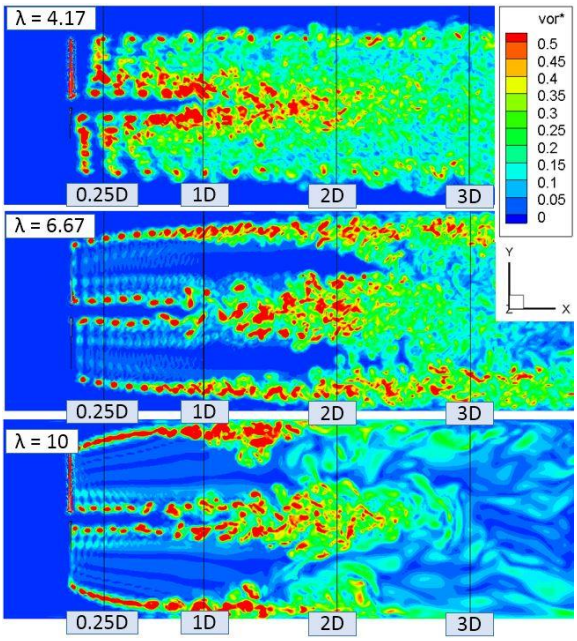

Figure 6. Vorticity contour of wake region(top: $\lambda = 4.17$, middle: $\lambda = 6.67$, bottom: $\lambda = 10$).

4.2. Velocity distribution

4.2.1. Frame of reference.

Next, analysis about velocity fields of wake region is investigated. Besides axial velocities, the radial flows and rotational flows behind the rotor plane should be investigated because they are supposed to represent the dynamics of rotational blade. Radial flows must correspond to radial expansion of the tip vortices shown in figure 4. And rotational flows of wake can be generated by the reaction force of blades. To visualize them, the Cartesian velocities (v, w) was converted into cylindrical velocities, as shown in figure 7; subsequently, the radial velocity V_r (1) and azimuthal velocity V_ψ (2) are derived. V_r and V_ψ can represent radial expansion and rotational flow of wake region respectively.

$$V_r = v \sin\psi + w \cos\psi \quad (1)$$

$$V_\psi = v \cos\psi - w \sin\psi \quad (2)$$

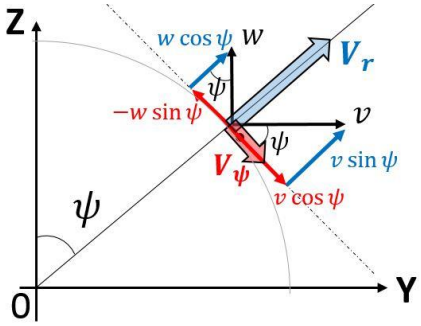

Figure 7. Rotating reference frame

4.2.2. Wake recovery process.

Characteristics of wake flow can be visualised by using a rotational reference frame. At First, the axial velocity contours of wake region are shown in figure 8. It is seen that when TSR increases, the velocity deficit also becomes quite significant. This phenomenon is caused by an increase in thrust. Associated cross-sectional contours of axial velocity (at x = 0.25D, 1D and 2D) are shown in figure 9. In the case of $\lambda = 4.17$, the region of velocity deficit is not expanded toward the radial direction, with associated distributions remaining essentially constant through each position. In contrast, for the cases of $\lambda = 6.67$ and $\lambda = 10$, the region of velocity deficit is notably expanded, with the axial velocity consequently decreasing in a manner similar to a tube-flow scenario. Furthermore, main stream mixing occurs by an exchange of momentum with radial and azimuthal velocities.

The distribution of V_r is shown in figure 10. The left column illustrates the plane at x = 0.25D as an example of the 'stable region' for the tip vortices in the case of $\lambda = 6.67$ and 10. These cases display a red circular area (i.e. a relatively strong radial flow toward the radial direction). Because of these radial velocities, wake expansion occurs. Micallef et al. [13] also pointed out that strong radial velocities exist near and around tip regions. Note that the strong red and blue regions represent cross sections of the tip vortices. In the case of $\lambda = 4.17$, the plane at x = 0.25D which can be affected by dynamic separation flow shows relatively weak radial flow. The planes at x = 2D represent the regions of vortex breakdown for each TSR. Because of the occurrence of tip vortex breakdown, small vortices are generated and diffused into the whole wake region, leading to the disappearance of radial flow. Alternatively, a wake expansion may cease, and in such a case, the tip vortex becomes unstable. As mentioned in the previous section, when TSR increases, the tip vortex breakdown process starts at an early stage; however, it should be noted that V_r correspondingly strengthens during the same period of time. Hence, the existence of V_r can act as a barrier that impedes recovery of the wake velocity because the existence of radial flow should prevent a wake from taking a main stream.

The azimuthal velocity (V_ψ), which stands for rotational movement of wake region is shown below in figure 11. As for $\lambda = 4.17$, which is the separated condition, the rotational flow is relatively weak and disappear quickly because of dynamic mixing by mid-span vortex, with the same tendency presenting itself for V_r. In terms of attached flow conditions, rotational flow is maintained until x = 1~2D which is much longer than the case of $\lambda = 4.17$. In comparison between $\lambda = 6.67$ and $\lambda = 10$, the case of $\lambda = 10$ displayed a rapid vortex breakdown and azimuthal velocity V_ψ disappears more rapidly. At x = 2D, the area depicting strong rotational flow essentially disappears. This indicates that tip vortex breakdown also corresponds to disappearance of azimuthal velocity. When comparing the position of disappearance for V_r and V_ψ, V_r tends to disappear earlier than V_ψ. If it is assumed that their disappearance has a direct correlation to mixing with the main stream, this tendency can be deemed conclusively valid because V_r distributes to the outside area, whereas V_ψ distributes inside of the wake. Therefore, V_r distributions that are close to the main stream tend to disappear more rapidly.

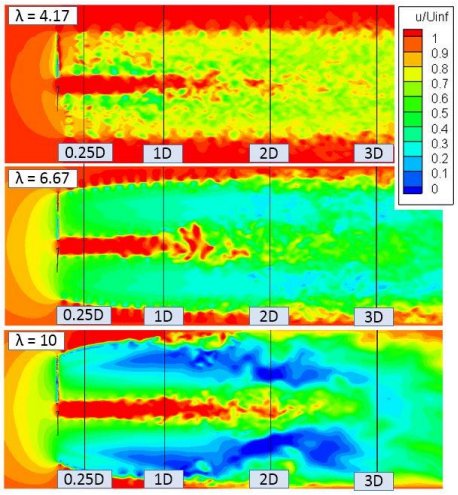

Figure 8. Axial velocity contour of wake region.

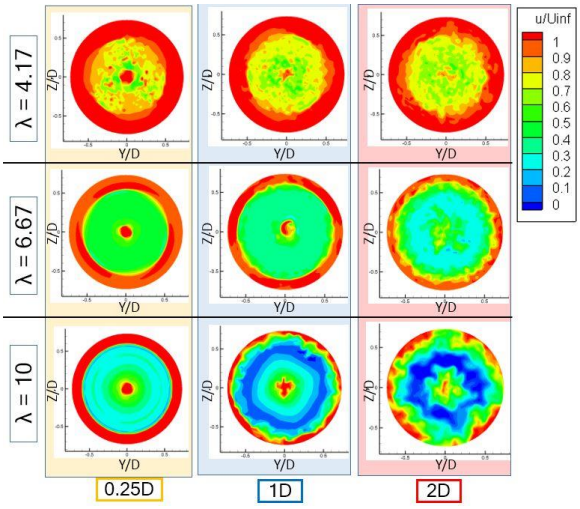

Figure 9. Axial velocity contours of wake (top: $\lambda = 4.17$, middle: $\lambda = 6.67$, bottom: $\lambda = 10$).

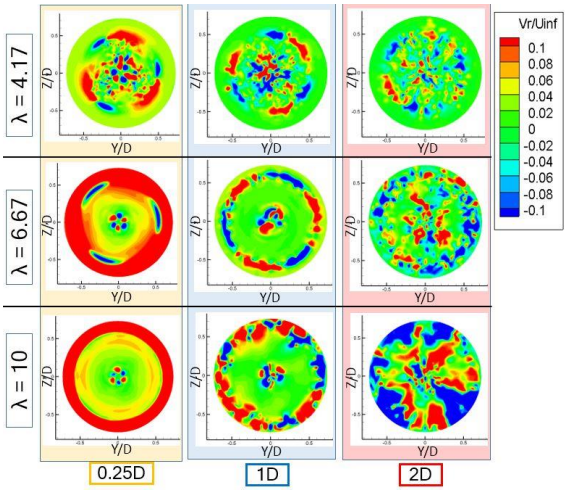

Figure 10. V_r contours of wake (top: $\lambda = 4.17$, middle: $\lambda = 6.67$, bottom: $\lambda = 10$).

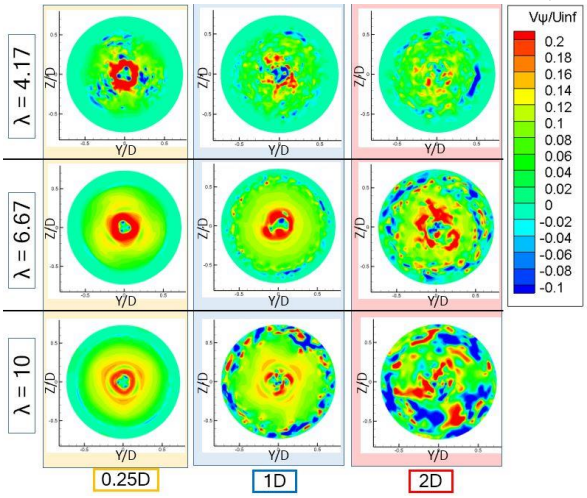

Figure 11. V_ψ contours of wake (top: $\lambda = 4.17$, middle: $\lambda = 6.67$, bottom: $\lambda = 10$).

5. Conclusion

URANS simulations and QDNS of the MEXICO rotor were executed by using rFlow3D and validations of the near-wake characteristics and axial force were implemented by comparing the results of the MEXICO projects. Furthermore, the effect of TSR on wake was investigated by focussing on the vorticity and velocities. From these results, the conclusions are following:

・The basic characteristics such as velocity distribution and axial force obtained by rFlow3D are generally consistent with the results of the MEXICO experiments.

・In low TSR, numerical conditions such as turbulence model need to be adjusted to predict the wake characteristics quantitatively.

・When TSR increases, the space between each vortex decreases. Therefore, the interaction between vortices increases and the tip vortex breakdown occurs more rapidly.

・During the beginning of vortex instabilities, wake expansion ceases because the radial flow produced by centrifugal forces disappears as a result of the breakdown of the tip vortices.

・Rapid breakdown of the tip vortices does not always correspond to rapid mixing of the wake with the main stream because this condition is often accompanied with a strong radial flow, which can be a barrier to wake mixing.

・Rotational flows by V_ψ tend to remain within the wake region longer than radial flows because the former primarily distribute inside of the wake, whereas radial flows typically exist in the outer area (proximal to the main stream).

6. Future works

To attain practical data, analytical conditions should approach actual field conditions. In particular, turbulence intensity is vital for accurately reproducing the actual phenomena; however, such simulations are normally difficult to duplicate and validate. Hence, via future studies, attempts will be set forth to conduct similar evaluations by comparing the attained results with light detection and ranging measurements.

References

[1] Uchida T, Ohya Y and Sugitani K 2006 Comparison between the wake behind wind turbine generator under optimal tip speed ratio and the wake behind stationary plate *Proc. of the 19th national symp. on wind engineering* pp187–92

[2] New Energy and Industrial Technology Development Organization 2008 *The guidebook for Installation of wind power energy*. http://www.nedo.go.jp/content/100079735 (2016/04/13 accessed)

[3] Vermeer L, Sørensen J and Crespo A 2003 Wind turbine wake aerodynamics *Prog. Aerosp. Sci.* **39** 467–510

[4] N Troldborg, F Zahle, PE Réthoré, N Sørensen 2012 Comparison of the wake of different types of wind turbine CFD models *50th AIAA Aerospace Sciences Meeting including the New Horisons Forum and Aerospace Exposition* 2012-0237

[5] AM AbbelSalam, V Ramalingam, 2013 Wake prediction of horizontal-axis wind turbine using full-rotor *Journal of Wind Engineering and industrial Aerodynamics* **124** 7-19

[6] Y Li, AM Castro, T Sinokrot, W Prescott, PM Carrica 2015 Coupled multi-body dynamics and CFD for wind turbine simulation includeing explicit wind turbulence *Renewable Energy* **76**: 338-361

[7] N Sezer-Uzol and O Uzol 2013 Effect of steady and transient wind shear on the wake structure and performance of a horizontal axis wind turbine rotor *Wind Energy* **16** pp 1-17

[8] T Göçmen, *et al.* 2016 Wind turbine wake models developed at the technical university of Denmark: A review *Renewable and Sustainable Energy Reviews* **60** pp 752-769

[9] Schepers JG, *et al*. 2012 *Final report of IEA Wind Task 29: Mexnext* (Phase 1) ECN-E 12-004

[10] Schepers JG, *et al*. 2014 *Final report of IEA Wind Task 29: Mexnext* (Phase 2) ECN-E 14-060

[11] Schepers JG and Snel H 2008 *Model Experiments in Controlled Conditions Final Report* ECN-E 07-042
[12] Schepers JG and Boorsma K 2014 *New MEXICO experiment* ECN-E 14-048
[13] Micallef D, Bussel G, Ferreira CS and Sant T 2012 An investigation of radial velocities for a horizontal axis wind turbine in axial and yawed flows. *Wind Energy* **16** 529–44
[14] Carrión M, Steijl R, Woodgate M, Barakos G, Manduate X and Gomez–Iradi S 2015 Computational fluid dynamics analysis of the wake behind the MEXICO rotor in axial flow conditions *Wind Energy* **18** 1023–45
[15] PE Réthoré, *et al*. 2011 MEXICO wind tunnel and wind turbine *29th AIAA Applied Aerodynamics Conf.* pp 2011–3373
[16] Tanabe Y and Saito S 2009 Significance of all-speed scheme in application to rotorcraft cfd simulations *The 3rd Int. Basic Research Conf. on Rotorcraft Technology*
[17] Shima E and Kitamura K 2009 On new simple low-dissipation scheme of AUSM-family for all speeds *AIAA paper* **136** pp 1–15
[18] Tanabe Y, Aoyama T, Oe H, Uemura Y and Sugawara H 2015 Simulations of horizontal Axis Wind Turbines in Complex Operational Conditions *The AHS 71st Annual Forum*
[19] JP Boris, FF Grinstein, ES Oran and RL Kolbe 1992 New insights into large eddy simulation *Fluid Dynamics Research* **10** pp 199–229
[20] Spalart PR and Allmaras SR 1992 A one-equation turbulence model for aerodynamic flows *AIAA J.* **92** 0439
[21] A Bechmann and NN Sørensen and F Zahle 2011 CFD simulations of the MEXICO rotor *Wind Energy* **14** pp 677–689